

# Diagnostic Criteria on $^{18}\text{F}$ -FDG PET/CT for Differentiating Benign from Malignant Focal Hypermetabolic Lesions of Parotid Gland

Soo Bin Park · Joon Young Choi · Eun Jeong Lee ·  
Jang Yoo · Miju Cheon · Suk Kyong Cho ·  
Yearn Seong Choe · Kyung-Han Lee · Byung-Tae Kim

Received: 11 May 2011 / Revised: 18 March 2012 / Accepted: 21 March 2012 / Published online: 21 April 2012  
© Korean Society of Nuclear Medicine 2012

## Abstract

**Purpose** We investigated PET/CT diagnostic criteria for differentiating benign from malignant parotid lesions with focal  $^{18}\text{F}$ -FDG uptake.

**Methods** The subjects of the study were 272 patients who exhibited focal  $^{18}\text{F}$ -FDG uptake of the parotid gland. Sixty-eight pathologically confirmed parotid lesions from 67 patients were included. The maximum SUV (SUVmax), uptake patterns (homogeneous vs. heterogeneous), size measured by CT, maximum Hounsfield units (HUmax) and margins on CT (well vs. ill defined) of each parotid lesion on PET/CT images were compared with final diagnoses.

**Results** Thirty-two parotid lesions were histologically proven to be malignant. There were significant differences in uptake patterns (cancer incidence, heterogeneous:homogeneous=79.2%:29.5%,  $p<0.0001$ ) and margins on CT (cancer incidence, ill:well defined=84.4%:13.3%,  $p<0.0001$ ) between benign and malignant lesions. The cancer risks of parotid lesions were 89.5% with heterogeneous uptake and ill-defined margins, 70.6% with heterogeneous uptake or ill-defined margins (no overlap in subjects) and 9.3% with homogeneous uptake and well-defined margins ( $p<0.0001$ ). When any lesion with heterogeneous uptake or ill-defined

margins was regarded as malignant, the sensitivity, specificity, positive predictive value, negative predictive value and accuracy were 90.6% (29/32), 80.6% (29/36), 80.6% (29/36), 90.6% (29/32) and 85.6% (58/68), respectively. For predicting malignancy, combined PET/CT criteria showed better sensitivity, NPV and accuracy than PET-only criteria, and had a tendency to have more accurate results than CT-only criteria. There were no significant differences in SUVmax, size or HUmax between benign and malignant lesions.

**Conclusion** Uptake patterns and margins on CT are useful PET/CT diagnostic criteria for differentiating benign from malignant lesions.

**Keywords** F-FDG · PET · PET/CT · Parotid gland · Cancer

## Introduction

Parotid gland neoplasms are rare, accounting for less than 3% of head and neck neoplasms [1]. Approximately one-fourth of all parotid tumors are malignant [2]. Many parotid neoplasms are considered to be borderline tumors, since they vary widely in histopathological appearance [3]. The complexity of parotid gland tumors is well described by the second revision of the WHO classification of salivary gland tumors, which includes almost 40 different types of epithelial tumors [4]. Parotid neoplasms exhibit a wide range of morphologies among individual tumors as well as within individual tumor masses. Therefore, it is difficult to make precise diagnoses by small incisional biopsies, and it is necessary to correlate clinical and radiological features [5].

$^{18}\text{F}$ -Fluorodeoxyglucose PET/CT ( $^{18}\text{F}$ -FDG PET/CT) is highly sensitive for the diagnosis of head and neck neoplasms, especially squamous cell carcinoma. However, there

**Electronic supplementary material** The online version of this article (doi:10.1007/s13139-012-0135-y) contains supplementary material, which is available to authorized users.

S. B. Park · J. Y. Choi (✉) · E. J. Lee · J. Yoo · M. Cheon ·  
S. K. Cho · Y. S. Choe · K.-H. Lee · B.-T. Kim  
Department of Nuclear Medicine, Samsung Medical Center,  
Sungkyunkwan University School of Medicine,  
50 Irwon-dong, Gangnam-gu,  
Seoul 135-710, Republic of Korea  
e-mail: jynm.choi@samsung.com

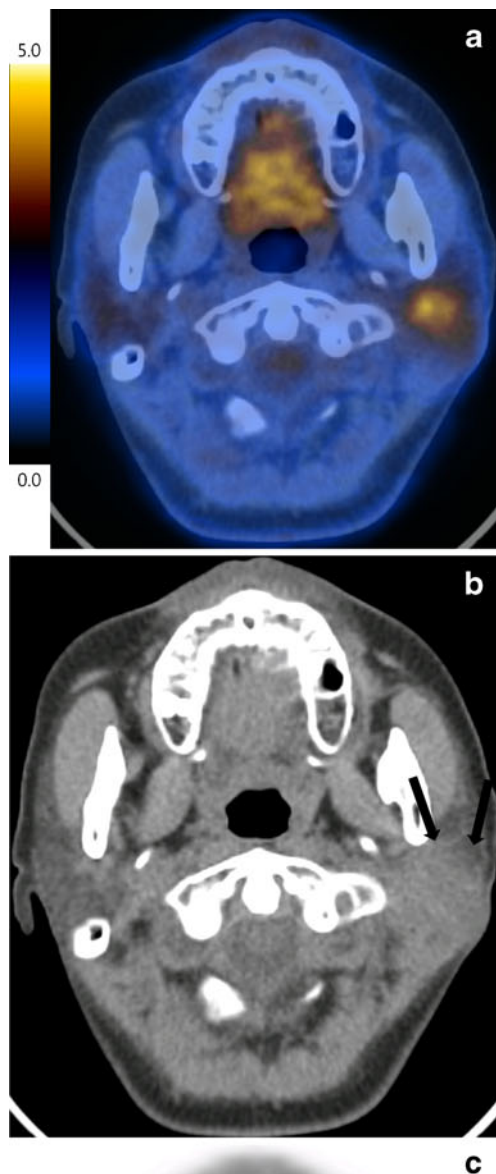


**Fig. 1** Fused PET/CT image of a 59-year-old female patient with a mass and pain in the left parotid area demonstrated a hypermetabolic mass in her left parotid gland (SUVmax=4.3) (a). The mass had an ill-defined margin on the CT image and the border was blurred, and it was not finely distinguished from normal parotid gland (arrow) (b), and heterogeneous uptake on PET image (c), which was proven to be mucoepidermoid carcinoma via left total parotidectomy

is controversy about the diagnostic value of  $^{18}\text{F}$ -FDG PET or PET/CT to classify parotid gland neoplasms as benign or malignant, because benign as well as malignant parotid tumors frequently have high  $^{18}\text{F}$ -FDG uptake [6–9]. In addition, diffusely and bilaterally increased  $^{18}\text{F}$ -FDG uptake of the parotid glands on PET/CT could either be a normal variant or may signify underlying inflammation [10].

To overcome these disadvantages, a recent study demonstrated that combined noncontrast CT is essential for improving the diagnostic accuracy of PET/CT for parotid masses [11]. However, the resulting low sensitivity and positive predictive values of less than 60% were problematic for routine clinical use. Therefore, the optimal PET/CT criteria for differentiating benign from malignant parotid lesions have yet to be established. The aim of the present study was to identify the specific PET/CT criteria that can help differentiate benign from malignant parotid lesions with focal  $^{18}\text{F}$ -FDG uptake.

## Subjects and Methods

### Subjects

We conducted a database search of medical records in our institution to identify patients with focal parotid uptake. A total of 32,477 patients were evaluated with whole-body  $^{18}\text{F}$ -FDG PET/CT from April 2003 to May 2009, including 28,772 patients (88.6%) who were evaluated for assessment of known or suspected malignancy and 3,705 healthy subjects (11.4%) who received PET scans for cancer screening. Of the 32,477 patients, 272 (0.8%) had focal  $^{18}\text{F}$ -FDG uptake of the parotid gland. Among these, patients with previous surgical history because of parotid tumors or without subsequent histological confirmation of focal parotid uptake were excluded from the analysis. Finally, 68 pathologically confirmed focal parotid lesions from 67 patients (47 men, 20 women; mean age,  $61.1 \pm 12.8$  years; age range, 19–84 years) by aspiration biopsy in 34, gun biopsy in 1, excision biopsy in 2 and parotidectomy in 31 patients were included in this study. Among them, 22 underwent PET/CT studies for suspected parotid tumors. In the remaining 45 patients, focal  $^{18}\text{F}$ -FDG uptake of the parotid gland was incidentally found (44 suspicious or known cases of non-parotid cancer, 1 for cancer screening). The ethics committee

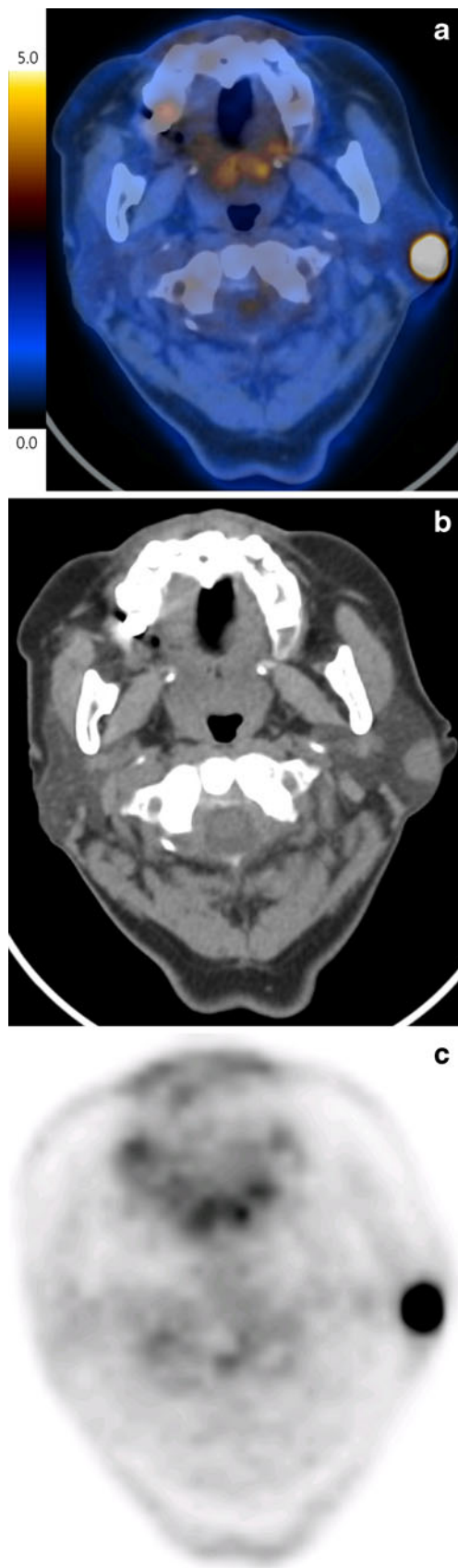


**Fig. 2** Incidental focal  $^{18}\text{F}$ -FDG uptake ( $\text{SUV}_{\text{max}}=18.8$ ) in the left parotid gland was found in a 75-year-old female subject undergoing PET/CT for the metastatic evaluation of her stomach cancer (**a**). The hypermetabolic parotid mass had a well-defined margin on CT image (**b**) and homogeneous uptake on PET image (**c**), and was proven to be Warthin's tumor via fine-needle aspiration biopsy

of our institution reviewed and approved the protocol of this retrospective study.

#### PET/CT Imaging

All subjects fasted for at least 6 h before PET/CT scans. Blood glucose levels at the time of injection of  $^{18}\text{F}$ -FDG were lower than 200 mg/dl in all patients. PET/CT scans were performed on two different dedicated PET/CT scanners (Discovery LS or Discovery STe, GE Healthcare, Milwaukee, WI, USA). Among the 67 patients, scans in 42 patients were performed using the Discovery LS PET/CT scanner, and scans in 25 patients were performed using the Discovery STe PET/CT scanner. No intravenous or oral contrast materials were used. In the Discovery LS scanner, whole-body CT was performed by a continuous spiral technique using an 8-slice helical CT (140 KeV, 40–120 mAs adjusted to the patients' body weight, section width of 5 mm) 45 min after the injection of  $\sim 370$  MBq  $^{18}\text{F}$ -FDG. After the CT scans were complete, emission scans were obtained from thigh to head for 4 min per frame in 2D mode. Attenuation-corrected PET images (voxel size= $4.3 \times 4.3 \times 3.9$  mm) were reconstructed using CT data by an ordered-subsets expectation maximization algorithm (28 subsets, 2 iterations). In the Discovery STe scanner, whole-body CT was performed by a continuous spiral technique using a 16-slice helical CT (140 KeV, 30–170 mAs with an AutomA mode, section width of 3.75 mm) 60 min after the injection of  $^{18}\text{F}$ -FDG (5.5 MBq/kg). After the CT scans were complete, emission scans were obtained from thigh to head for 2.5 min per frame in 3D mode. Attenuation-corrected PET images (voxel size= $3.9 \times 3.9 \times 3.3$  mm) were reconstructed using CT data by a 3D ordered-subset expectation maximization algorithm (20 subsets, 2 iterations). Commercial software (Xeleris, GE Healthcare) was used to accurately coregister the separate CT and PET scan data.

#### Image Analysis

PET/CT images were visually and semi-quantitatively interpreted by two nuclear medicine physicians who reached consensus. We reviewed PET/CT images focusing on abnormal focal  $^{18}\text{F}$ -FDG uptake in the parotid gland. Image interpretations of focal parotid lesions concentrated on maximum SUV ( $\text{SUV}_{\text{max}}$ ) and  $^{18}\text{F}$ -FDG uptake patterns on the PET images and size, maximum Hounsfield units ( $\text{HU}_{\text{max}}$ ) and margins on noncontrast CT images. In this study, focal parotid lesions

were defined as focally increased  $^{18}\text{F}$ -FDG uptake on PET images that could be distinguished from background parotid gland tissues. SUVmax measurements were acquired according to attenuation-corrected images, amounts of injected  $^{18}\text{F}$ -FDG, the body weight of each patient, and cross-calibration factors between the PET and the dose calibrator.  $^{18}\text{F}$ -FDG uptake patterns were defined as homogeneous or heterogeneous with SUV 5.0 as an upper window threshold. Margins were evaluated as well- or ill-defined. If the focal parotid lesions showed spicular margins, indistinct borders or invasion into adjacent tissues, they were considered to have ill-defined margins. If margins clearly showed either nodular or lobular shapes, they were considered to have well-defined margins with none of the findings of ill-defined margins (Figs. 1, 2).

### Statistical Analysis

Statistical analyses were performed using a commercial software program (PASW Statistics 18, IBM Corp., Somers, NY, USA). Pearson's chi-square tests and Mann–Whitney tests were used to compare PET/CT findings between benign and malignant focal parotid lesions.  $P$  values  $<0.05$  were considered statistically significant. Numerical data were expressed as mean  $\pm$  SD.

### Results

Among the 68 focal parotid lesions from the 67 patients, 32 lesions (47%) from 32 patients were histologically proven to be malignant (metastatic carcinoma in 11, mucoepidermoid carcinoma in 8, salivary ductal carcinoma in 3, adenocarcinoma in 3, adenoid cystic carcinoma in 2 and other in 5). The remaining 36 lesions (53%) from 35 patients were histologically proven to be benign (Warthin's tumor in 24, pleomorphic adenoma in 4, inflammation in 4 and other in 4).

Table 1 compares the clinical and PET/CT findings between benign and malignant focal parotid lesions. There were significant differences in  $^{18}\text{F}$ -FDG uptake patterns and margins on CT between benign and malignant parotid lesions. However, there were no significant differences in SUVmax, size by CT, and HUm<sub>ax</sub> between benign and malignant parotid lesions. The risks of malignancy for focal parotid lesions with heterogeneous  $^{18}\text{F}$ -FDG uptake were higher than homogeneous  $^{18}\text{F}$ -FDG uptake [79.2% (19/24) vs. 29.5% (13/44)], and those for ill-defined CT margins were higher than for well-defined CT margins [84.4% (27/32) vs. 15.6% (5/32)]. By combining these two PET/CT findings, the risk of malignancy for focal parotid lesions with both heterogeneous  $^{18}\text{F}$ -FDG uptake and ill-defined CT margins was 89.5% (17/19), for either heterogeneous FDG uptake or ill-

**Table 1** Comparisons of clinical and PET/CT findings between benign and malignant focal parotid lesions detected on  $^{18}\text{F}$ -FDG PET/CT

|                               | Benign<br>(n=36)            | Malignant<br>(n=32)         | $P$<br>value | Odds<br>ratio |
|-------------------------------|-----------------------------|-----------------------------|--------------|---------------|
| Age (years)                   | 65.4 $\pm$ 11.3             | 58.6 $\pm$ 11.9             | NS           |               |
| Sex (male/female)             | 28/8                        | 20/12                       | NS           |               |
| Maximum SUV                   | 11.0 $\pm$ 7.5              | 9.1 $\pm$ 7.7               | NS           |               |
| Uptake pattern                |                             |                             |              |               |
| Homogeneous/<br>heterogeneous | 31/5                        | 13/19                       | $<0.001$     | 9.1           |
| Size by CT (mm)               | 16.8 $\pm$ 7.8 <sup>a</sup> | 23.7 $\pm$ 1.8 <sup>b</sup> | NS           |               |
| Maximum<br>Hounsfield units   | 66.9 $\pm$ 1.4 <sup>c</sup> | 88.6 $\pm$ 7.2 <sup>d</sup> | NS           |               |
| Margin on CT                  |                             |                             |              |               |
| Well/ill defined              | 27/5 <sup>e</sup>           | 5/27                        | $<0.001$     | 35.1          |

NS not significant

<sup>a</sup> Seven cases were excluded because of beam-hardening artifacts or non-visualization on CT

<sup>b</sup> Three cases were excluded because of beam-hardening artifacts

<sup>c</sup> Thirteen cases were excluded because of beam-hardening artifacts or non-visualization on CT

<sup>d</sup> Seven cases were excluded because of beam-hardening artifacts

<sup>e</sup> Four cases were excluded because of beam-hardening artifacts or non-visualization on CT

defined CT margins was 70.6% (12/17), and for both homogeneous  $^{18}\text{F}$ -FDG uptake and well-defined CT margins was 9.3% (3/32) ( $p<0.001$ ).

Based on these results, heterogeneous  $^{18}\text{F}$ -FDG uptake or ill-defined CT margins of focal parotid lesions were adopted as combined PET/CT criteria for diagnosing malignancy. In four cases, whose CT margins were impossible to evaluate because of beam-hardening artifact, the  $^{18}\text{F}$ -FDG uptake criterion only was applied for the differential diagnosis. When using these criteria, PET/CT showed a sensitivity of 90.6% (29/32), specificity of 80.6% (29/36), positive predictive value of 80.6% (29/36), negative predictive value of 90.6% (29/32) and accuracy of 85.6% (58/68), respectively, for predicting malignancy, which showed better sensitivity, NPV and accuracy than PET-only diagnostic criteria with sensitivity of 59.4% (19/32,  $p=0.002$ ), NPV of 70.5% (31/44,  $p=0.033$ ) and accuracy of 73.5% (50/68,  $p<0.001$ ). There were no significant differences in specificity (80.6% vs. 86.1%,  $p=0.5$ ) and PPV (80.6% vs. 79.2%,  $p=0.895$ ) between combined PET/CT criteria and PET-only criteria. For predicting malignancy, our combined PET/CT criteria had the tendency to be more accurate than CT-only diagnostic criteria (85.6% vs. 79.4%,  $p=0.062$ ). There were no significant differences in sensitivity (90.6% vs. 84.4%,  $p=0.5$ ), specificity (80.6% vs. 84.4%,  $p=0.25$ ), PPV (80.6% vs. 84.4%,  $p=0.68$ ) and NPV (90.6% vs. 84.4%,  $p=0.45$ ) between combined PET/CT criteria and CT-only criteria.

**Table 2**  $^{18}\text{F}$ -FDG PET/CT findings of seven false-positive cases

| Pathology                                 | CT margin    | Uptake pattern | Size (cm) | SUVmax |
|---|--------------|----------------|-----------|--------|
| Abscess                                   | Ill defined  | Heterogeneous  | 6         | 15.3   |
| Pleomorphic adenoma                       | Ill defined  | Homogeneous    | 0.5       | 3.8    |
| Pleomorphic adenoma                       | Well defined | Heterogeneous  | 3         | 6      |
| Pleomorphic adenoma (containing necrosis) | Ill defined  | Heterogeneous  | 3.5       | 5.6    |
| Warthin's tumor                           | Ill defined  | Homogeneous    | 1.1       | 14.7   |
| Warthin's tumor                           | Well defined | Heterogeneous  | 3.2       | 19.3   |
| Warthin's tumor                           | Well defined | Heterogeneous  | 3.3       | 17.5   |

We detected three false-negative cases and seven false-positive cases when applying our combined diagnostic PET/CT criteria. All of the false-negative cases were metastatic parotid lesions from other primary malignancies (liver, pancreas and lung). The seven false-positive cases included one abscess, three pleomorphic adenomas and three Warthin's tumors. Table 2 shows the  $^{18}\text{F}$ -FDG PET/CT findings of these false-positive cases.

Table 3 shows the differences between primary parotid malignancies and metastatic parotid lesions; it was significantly different in  $^{18}\text{F}$ -FDG uptake patterns, size, HUmax and margins on CT. Among 11 cases of metastatic parotid lesions, there were no significant differences in SUVmax ( $10.2\pm 11.7$  vs.  $6.4\pm 3.1$ ) and size ( $15.2\pm 6.9$  vs.  $11.2\pm 2.0$ ) between true-positive and false-negative cases according to our combined diagnostic PET/CT criteria. Our combined PET/CT criteria are more sensitive in primary parotid malignancies than in metastatic parotid lesions.

**Table 3** Comparisons of PET/CT findings between primary parotid malignancies and metastatic parotid lesions detected on  $^{18}\text{F}$ -FDG PET/CT

|   | Primary (n=21)   | Metastasis (n=11) | P value | Odds ratio |
|---|------------------|-------------------|---------|------------|
| Maximum SUV                             | $9.1\pm 6.5$     | $9.5\pm 10.5$     | NS      |            |
| Uptake pattern                          |                  |                   |         |            |
| Homogeneous/heterogeneous               | 4/17             | 9/2               | 0.001   | 12.35      |
| Size by CT (mm)                         | $29.5\pm 10.3^a$ | $14.1\pm 6.2$     | <0.001  |            |
| Maximum Hounsfield units                | $91.9\pm 58.3^b$ | $84.5\pm 90.0$    | 0.003   |            |
| Margin on CT                            |                  |                   |         |            |
| Well/ill defined                        | 1/20             | 4/7               | 0.037   | 35.1       |
| Sensitivity of combined PET/CT criteria | 100% (21/21)     | 72.7% (8/11)      | 0.012   | 6.32       |

NS not significant

<sup>a</sup> Three cases were excluded because of beam-hardening artifacts or non-visualization on CT

<sup>b</sup> Seven cases were excluded because of beam-hardening artifacts or non-visualization on CT

## Discussion

This study demonstrated that both uptake patterns of  $^{18}\text{F}$ -FDG and margins of focal lesions on CT were essential diagnostic criteria for differentiating benign from malignant parotid lesions on PET/CT. Using these combined diagnostic criteria, PET/CT showed a good diagnostic accuracy of 85.6%, which was better than PET-only or CT-only diagnostic criteria.

Several studies have addressed the use of  $^{18}\text{F}$ -FDG PET for the differential diagnosis of parotid lesions [6, 7, 9, 11, 12]. However, when PET was used with SUV-based diagnostic criteria, there was so much overlap between the benign and malignant lesions that it failed to play a significant role in the differential diagnosis of benign from malignant parotid lesions because of low specificity (31–66%), positive predictive value (19.1–60%) and accuracy (33–69%) even though sensitivity was relatively high (75–100%).

This is the first study evaluating the use of both  $^{18}\text{F}$ -FDG uptake patterns and CT margins of focal parotid lesions on PET/CT for differentiating benign from malignant parotid lesions. Focal parotid lesions with heterogeneous  $^{18}\text{F}$ -FDG uptake were more likely to be malignant than those with homogeneous  $^{18}\text{F}$ -FDG uptake. The uptake patterns may change according to the window threshold SUVs of monitors. For the objective evaluation of uptake patterns, we used a fixed upper window threshold SUV of 5.0, which is the standard upper window threshold SUV for routine clinical PET interpretation in our institute. Intra-tumor  $^{18}\text{F}$ -FDG uptake in cancer cells may be heterogeneous due to several physiologic parameters such as perfusion, cell proliferation, tumor viability, aggressiveness, hypoxia or tumor necrosis [13, 14]. This may explain the good diagnostic results of uptake patterns observed in our study.

Focal parotid lesions with ill-defined margins on CT appeared to have higher risks of malignancy than lesions with well-defined margins on CT, in agreement with the results of another recently reported study [11]. Infiltrative growth to surrounding tissues is a hallmark of cancer, which corresponds to ill-defined margins on CT [15]. Although CT alone may not be able to differentiate between benign and malignant parotid lesions [16], the

results of our study suggest that information about CT margins improves diagnostic efficacy when combined with uptake patterns of  $^{18}\text{F}$ -FDG.

When parotid lesions with ill-defined CT margins or heterogeneous  $^{18}\text{F}$ -FDG uptake were identified as malignant according to our combined diagnostic PET/CT criteria, we detected three false-negative cases and seven false-positive cases. All false-negative cases were metastatic parotid lesions, which seemed to show relatively smaller size (9.2–13.2 mm) and lower SUVmax (3.3–9.5) than those of true-positive metastatic parotid lesions without statistically significant differences, partly because of the small number of subjects. Table 3 suggests that our combined diagnostic PET/CT criteria were more suitable for detecting primary parotid malignancies than metastatic parotid lesions because of high sensitivity of 100%.

Among the seven false-positive cases, five showed heterogeneous  $^{18}\text{F}$ -FDG uptake, and all of these lesions were larger ( $\geq 3$  cm) than false-positive cases with homogeneous  $^{18}\text{F}$ -FDG uptake. Although abscesses are benign parotid lesions, they were observed to have ill-defined CT margins in our study, which is in accordance with the results of a previous study indicating that parotid gland inflammation was also characterized by ill-defined margins on CT or MRI in 46.2% (6/13) of cases [12]. Although only 12.5% of Warthin's tumors (3/14) were identified as false positives using our combined PET/CT criteria, 75% of pleomorphic adenomas (3/4) showed false-positive results. This finding suggests that pleomorphic adenoma is the main cause of false-positive results when using our combined PET/CT criteria.

Among the 67 patients with pathologically confirmed focal parotid lesions, focal parotid lesions were incidentally found in 44 patients with suspicious or known non-parotid cancers. Among these, 13 patients (29.5%) were proven to have clinically unexpected malignant parotid lesions. This finding suggests that  $^{18}\text{F}$ -FDG PET/CT may be useful for screening cancer patients for unexpected malignant parotid lesions, which supports the results of a previous study suggesting that  $^{18}\text{F}$ -FDG PET/CT is useful for screening patients for second primary cancers or clinically unexpected distant metastases [17].

In accordance with the results of previous studies [6–8, 15], SUVmax was not useful for differentiating benign from malignant parotid lesions because of the wide range of SUVmax and high SUVmax of benign as well as malignant parotid lesions such as Warthin's tumor (mean SUVmax =  $11.8 \pm 5.0$ , SUVmax range = 5.1–19.3) and mucoepidermoid carcinoma (mean SUVmax =  $5.7 \pm 4.7$ , SUVmax range = 2.6–16.8). Although the nature and variation of  $^{18}\text{F}$ -FDG uptake in benign parotid tumors remain unclear, high  $^{18}\text{F}$ -FDG uptake may be related to high mitochondrial content and activity, especially for Warthin's tumors [15].

This study had several limitations. Because of its retrospective design, not all subjects with focal hypermetabolic parotid lesions underwent histological confirmation. This may have caused referral bias inflating the proportion of malignant parotid lesions in the sample (47%) [2]. Secondly, the CT margins of focal hypermetabolic parotid lesions were not evaluated in some patients because of beam-hardening artifacts of dental structures or non-visualization on non-contrast CT, which raises the potential of selection bias. The final possible limitation was the use of two different kinds of scanners and acquisition protocols, and the accompanying uncertainty of whether or not SUVmax measurements were consistent between the two scanners. However, when we analyzed SUVmax,  $^{18}\text{F}$ -FDG uptake patterns and margins on CT between benign and malignant parotid lesions, there were no significant differences in SUVmax values according to scanner, and the  $^{18}\text{F}$ -FDG uptake patterns and margins on CT still significantly differed in both scanner groups (Supplementary Table 1 and Table 2).

In conclusion, both  $^{18}\text{F}$ -FDG uptake patterns and margins of focal parotid lesions on CT are useful PET/CT diagnostic criteria for differentiating benign from malignant lesions.  $^{18}\text{F}$ -FDG PET/CT scans using these combined criteria may be helpful to identify patients with focal parotid lesions who require pathological confirmation because of their high sensitivity and negative predictive value.

**Conflict of interest** The authors have no conflicts of interest to declare.

## References

1. Eveson JW, Cawson RA. Salivary gland tumours. A review of 2410 cases with particular reference to histological types, site, age and sex distribution. *J Pathol.* 1985;146:51–8.
2. Devita Jr VT, Hellman S, Rosenberg S. *Cancer principles & practice of oncology.* 7th ed. Philadelphia, PA: Lippincott Williams & Wilkins; 2005. p. 722–6.
3. van der Wal JE, Leverstein H, Snow GB, Kraaijenhagen HA, van der Waal I. Parotid gland tumors: histologic reevaluation and reclassification of 478 cases. *Head Neck.* 1998;20:204–7.
4. Seifert G, Sobin L. WHO International histological classification of tumours. *Histological typing of salivary gland tumours.* 2nd ed. Heidelberg: Springer Verlag; 1991.
5. Speight PM, Barrett AW. Salivary gland tumours. *Oral Dis.* 2002;8:229–40.
6. Keyes Jr JW, Harkness BA, Greven KM, Williams DW, Watson NE, Frederick-Mcguirt W. Salivary gland tumors: pretherapy evaluation with PET. *Radiology.* 1994;192:99–102.
7. Uchida Y, Minoshima S, Kawata T, Motoori K, Nakano K, Kazama T, et al. Diagnostic value of FDG PET and salivary gland scintigraphy for parotid tumors. *Clin Nucl Med.* 2005;30:170–6.
8. Okamura T, Kawabe J, Koyama K, Ochi H, Yamada R, Sakamoto H, et al. Fluorine-18 Fluorodeoxyglucose positron emission

- tomography imaging of parotid mass lesions. *Acta Otolaryngol Suppl.* 1998;538:209–13.
9. Rubello D, Nanni C, Castellucci P, Rampin L, Farsad M, Franchi R, et al. Does 18F-FDG PET/CT play a role in the differential diagnosis of parotid masses. *Panminerva Med.* 2005;47:187–9.
  10. Basu S, Houseni M, Alavi A. Significance of incidental fluorodeoxyglucose uptake in the parotid glands and its impact on patient management. *Nucl Med Commun.* 2008;29:367–73.
  11. Wang H, Zuo C, Hua F, Huang Z, Tan H, Zhao J, et al. Efficacy of conventional whole-body <sup>18</sup>F-FDG PET/CT in the incidental findings of parotid masses. *Ann Nucl Med.* 2010;24:571–7.
  12. Ozawa N, Okamura T, Koyama K, Nakayama K, Kawabe J, Shiomi S, et al. Retrospective review: usefulness of a number of imaging modalities including CT, MRI, technetium-99 m pertechnetate scintigraphy, gallium-67 scintigraphy and F-18-FDG PET in the differentiation of benign from malignant parotid masses. *Radiat Med.* 2006;24:41–9.
  13. Tixier F, Rest CCL, Hatt M, Albarghach N, Pradier O, Metges JP, et al. Intratumor heterogeneity characterized by textural features on baseline <sup>18</sup>F-FDG PET images predicts response to concomitant radiochemotherapy in esophageal cancer. *J Nucl Med.* 2011;52:369–78.
  14. Basu S, Kwee TC, Gatenby R, Sabuory B, Torigian DA, Alavi A. Evolving role of molecular imaging with PET in detecting and characterizing heterogeneity of cancer tissue at the primary and metastatic sites, a plausible explanation for failed attempts to cure malignant disorders. *Eur J Nucl Med Mol Imaging.* 2011. doi:10.1007/s00259-011-1787-z.
  15. Frederick-Mcguirt W, Keyes Jr JW, Greven KM, Williams III DW, Watson Jr NE, Cappellari JO. Preoperative identification of benign versus malignant parotid masses: a comparative study including positron emission tomography. *Laryngoscope.* 1995;105:579–84.
  16. Berg HM, Jacobs JB, Kaufman D, Reede DL. Correlation of fine needle aspiration biopsy and CT scanning of parotid masses. *Laryngoscope.* 1986;96:1357–62.
  17. Choi JY, Lee KS, Kwon OJ, Shim YM, Baek CH, Park K, et al. Improved detection of second primary cancer using integrated [<sup>18</sup>F] fluorodeoxyglucose positron emission tomography and computed tomography for initial tumor staging. *J Clin Oncol.* 2005;23:7654–9.